

Grenzflächenverfahrenstechnik II

7. Vorlesung

31. Januar 2020

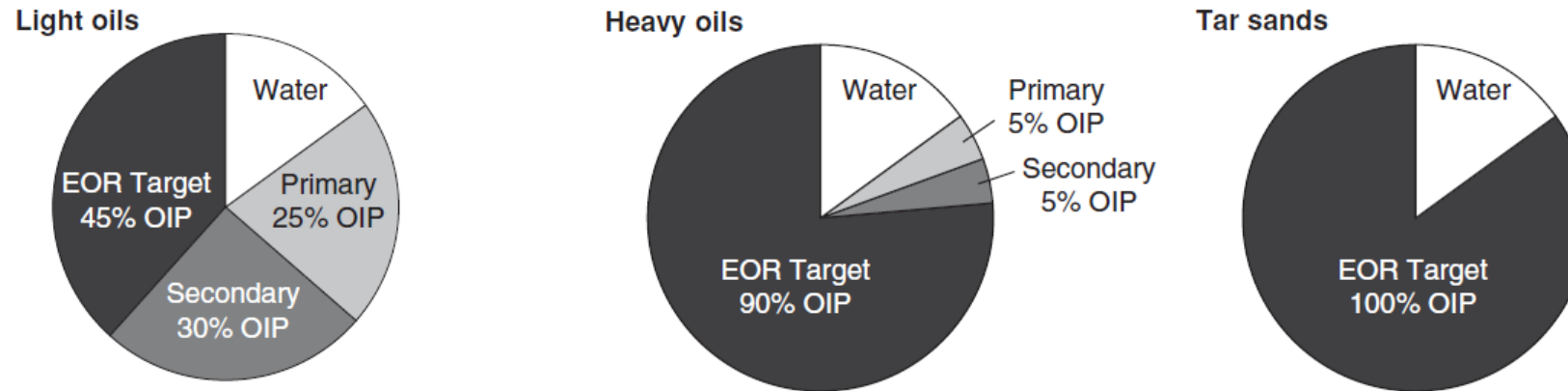
Dr. sMartinterface Rudolph

Inhalt der Lehrveranstaltung

- 0 Einführung
- 1 Grundlagen der Benetzung
- 2 Spreitungskoeffizient
- 3 Adhäsions-/Kohäsionsarbeit
- 4 Kontaktwinkelhysterese
- 5 Messung an Partikelsystemen
- 6 Dimensionslose Kennzahlen
- 7 Partikel in Fluiden-Grenzflächen
- 8 **Applikationen**

8 Applikationen

8.1 (Surfactant) Enhanced Oil Recovery



(Assuming $S_{oi} = 85\% \text{ PV}$ and $S_w = 15\% \text{ PV}$)

Figure 1
EOR target for different hydrocarbons.

8 Applikationen

8.1 (Surfactant) Enhanced Oil Recovery

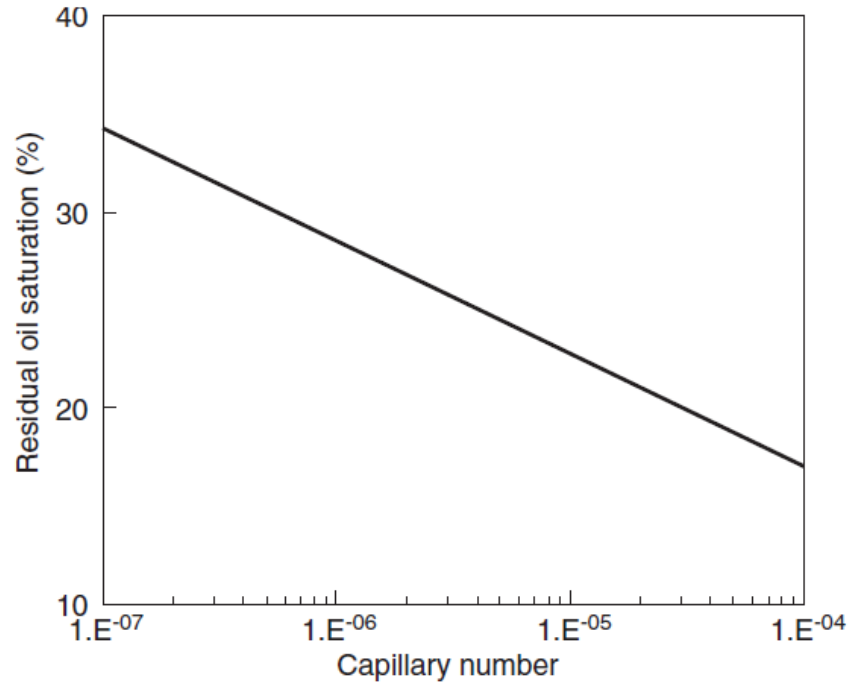


Figure 2
Effect of capillary number on residual oil saturation.

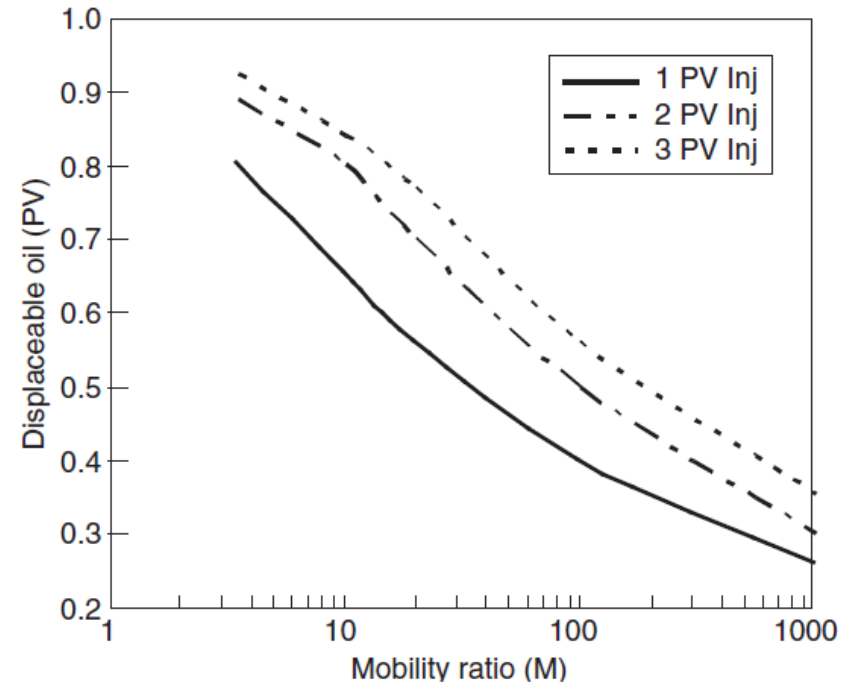


Figure 3
Effect of mobility ratio on displaceable oil.

8 Applikationen

8.1 (Surfactant) Enhanced Oil Recovery

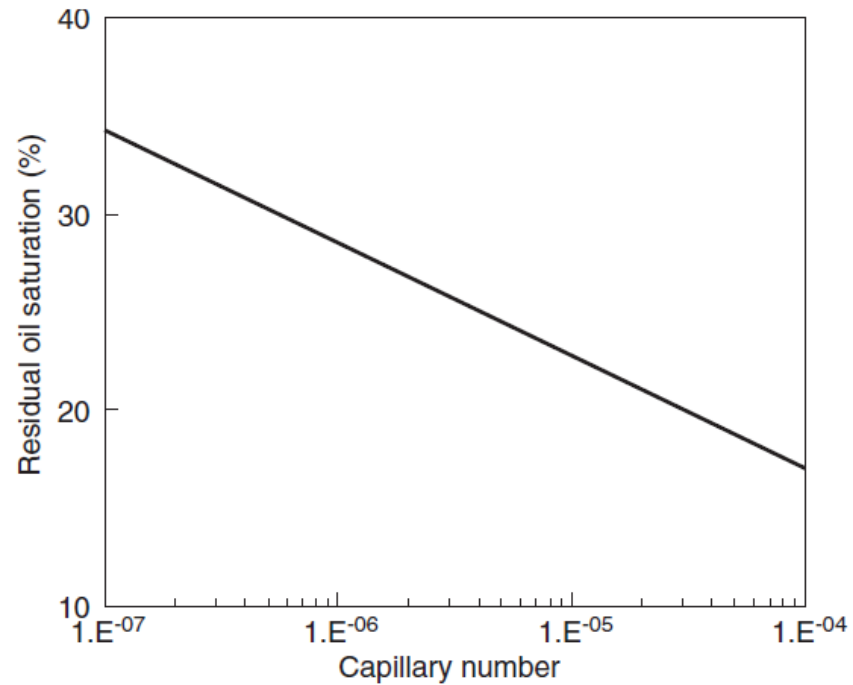


Figure 2
Effect of capillary number on residual oil saturation.

$$N_C = \frac{v \cdot \mu}{\gamma}$$

8 Applikationen

8.1 (Surfactant) Enhanced Oil Recovery

Mobility ratio is defined as $M = \lambda_{ing} / \lambda_{ed}$, where λ_{ing} is the mobility of the displacing fluid (e.g. water), and λ_{ed} is the mobility of the displaced fluid (oil). ($\lambda = k/\mu$, where k is the effective permeability, (m²) and μ is the viscosity (Pa.s) of the fluid concerned). Mobility ratio influences the microscopic (pore level) and macroscopic (areal and vertical sweep) displacement efficiencies. A value of $M > 1$ is considered unfavourable, because it indicates that the displacing fluid flows more readily than the displaced fluid (oil), and it can cause channelling of the displacing fluid, and as a result, bypassing of some of the residual oil. Under such conditions, and in the absence of viscous instabilities, more displacing fluid is needed to obtain a given residual oil saturation. The effect of mobility ratio on displaceable oil is shown in Figure 3, the data for which was obtained from calculations using Buckley-Leverett theory for waterflooding. The three curves represent 1, 2 and 3 pore volumes of total fluid injected, respectively. Displacement efficiency is increased when $M = 1$, and is denoted a “favourable” mobility ratio.

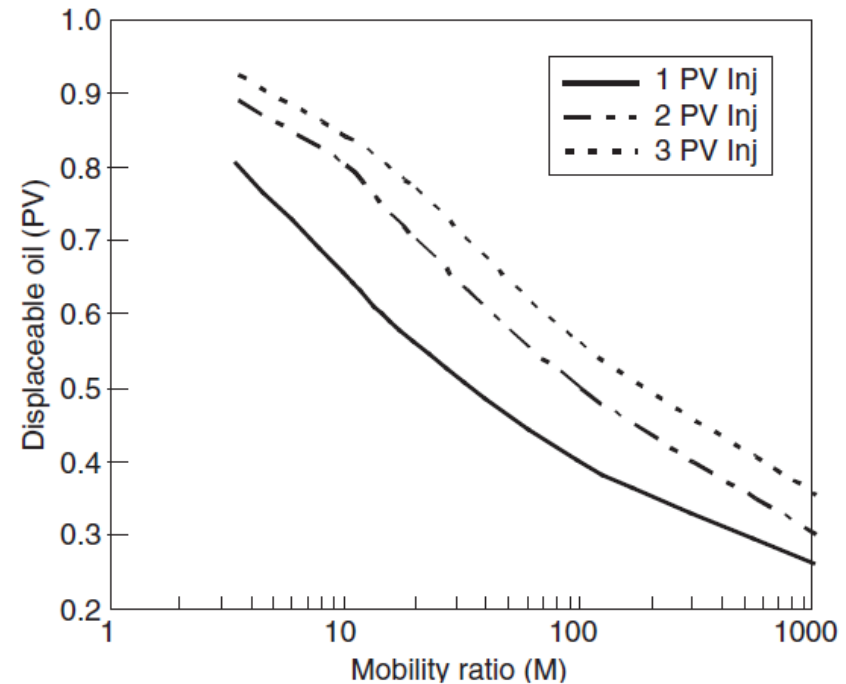
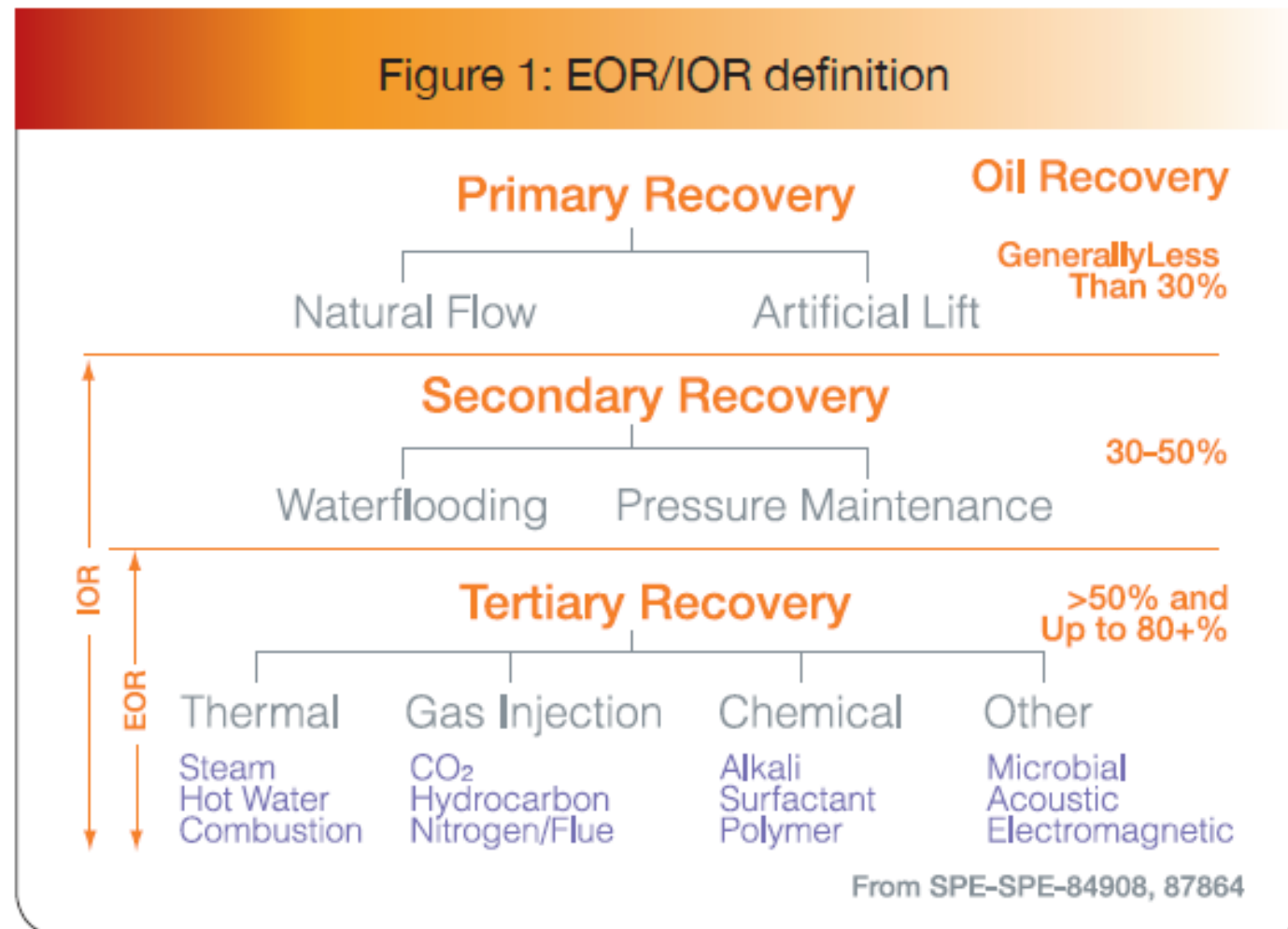


Figure 3
Effect of mobility ratio on displaceable oil.

8 Applikationen

8.1 (Surfactant) Enhanced Oil Recovery



8 Applikationen

8.1 (Surfactant) Enhanced Oil Recovery

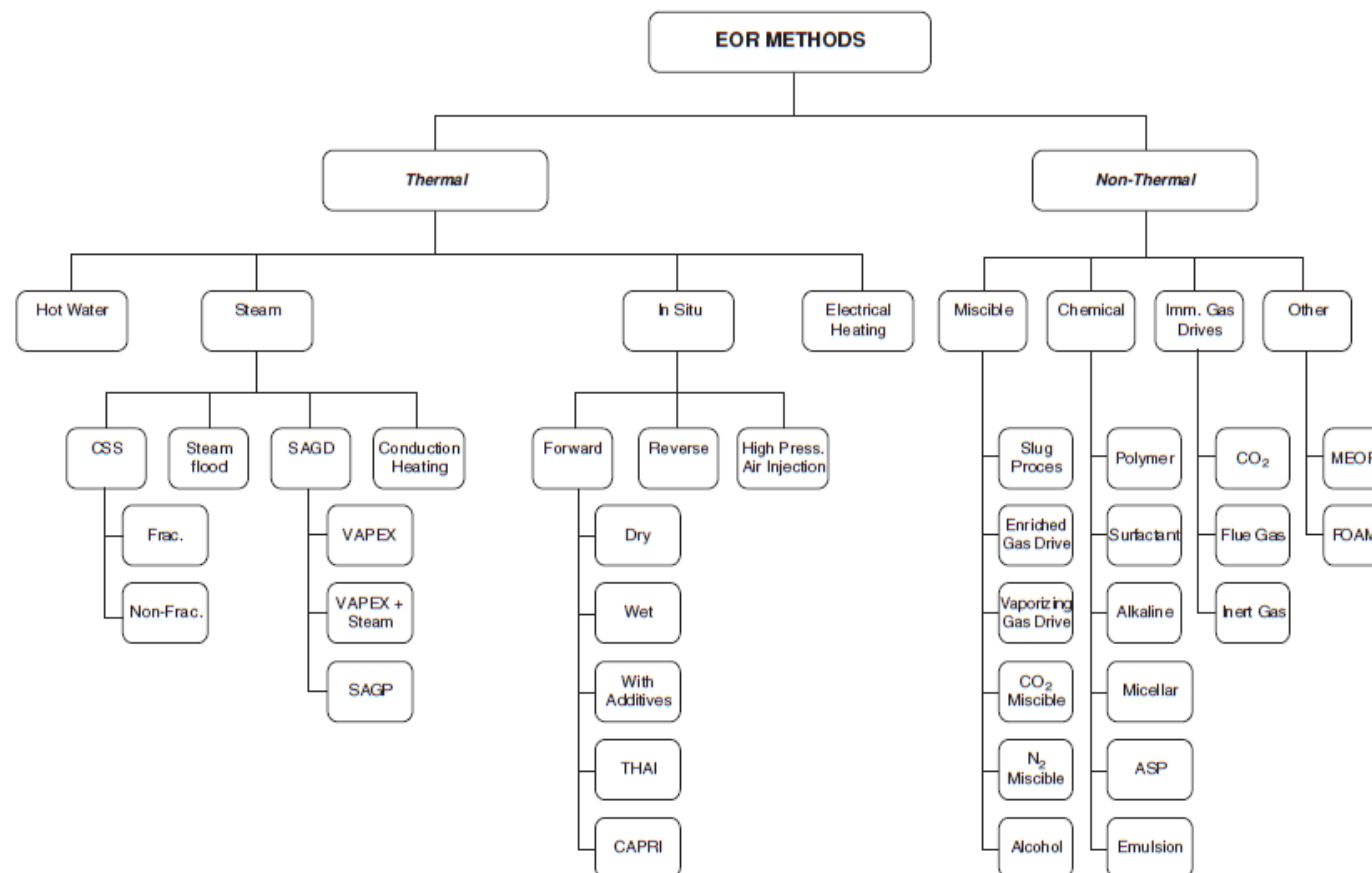
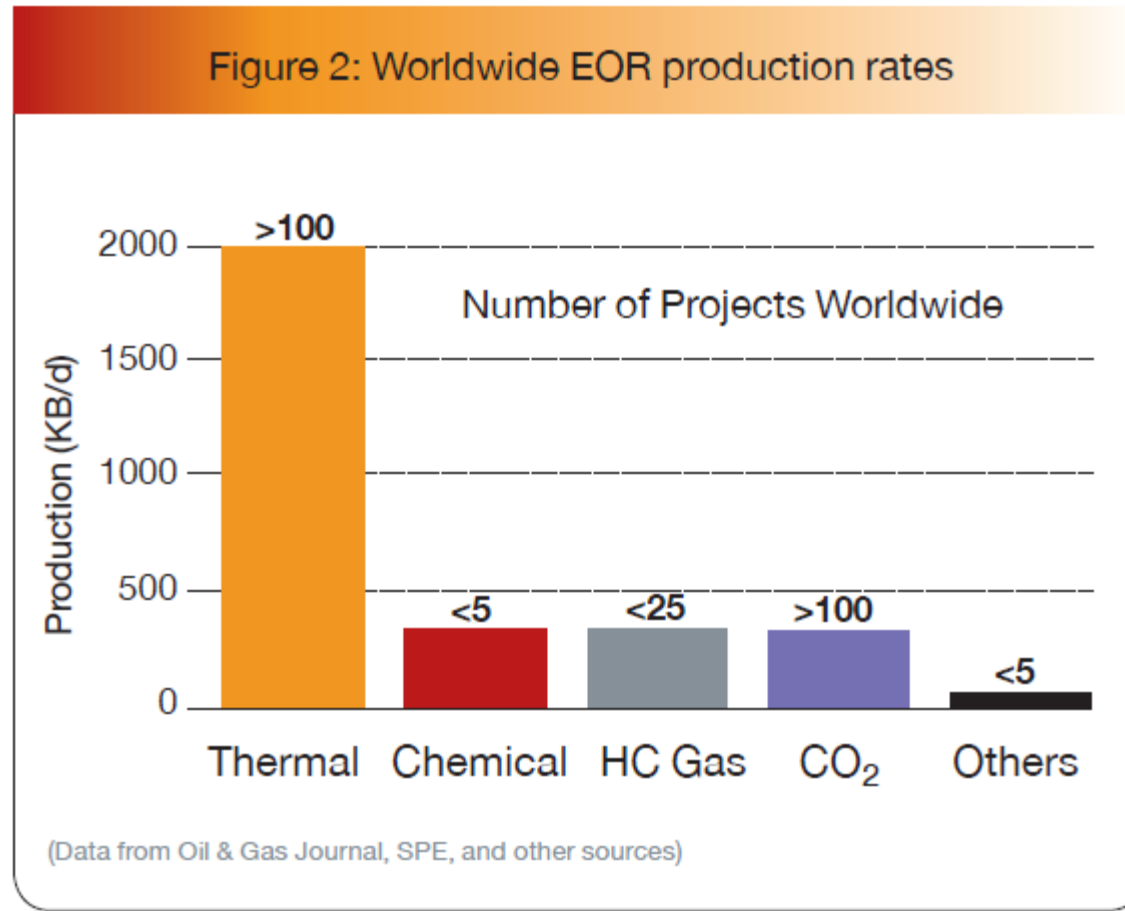


Figure 4
Classification of EOR methods.

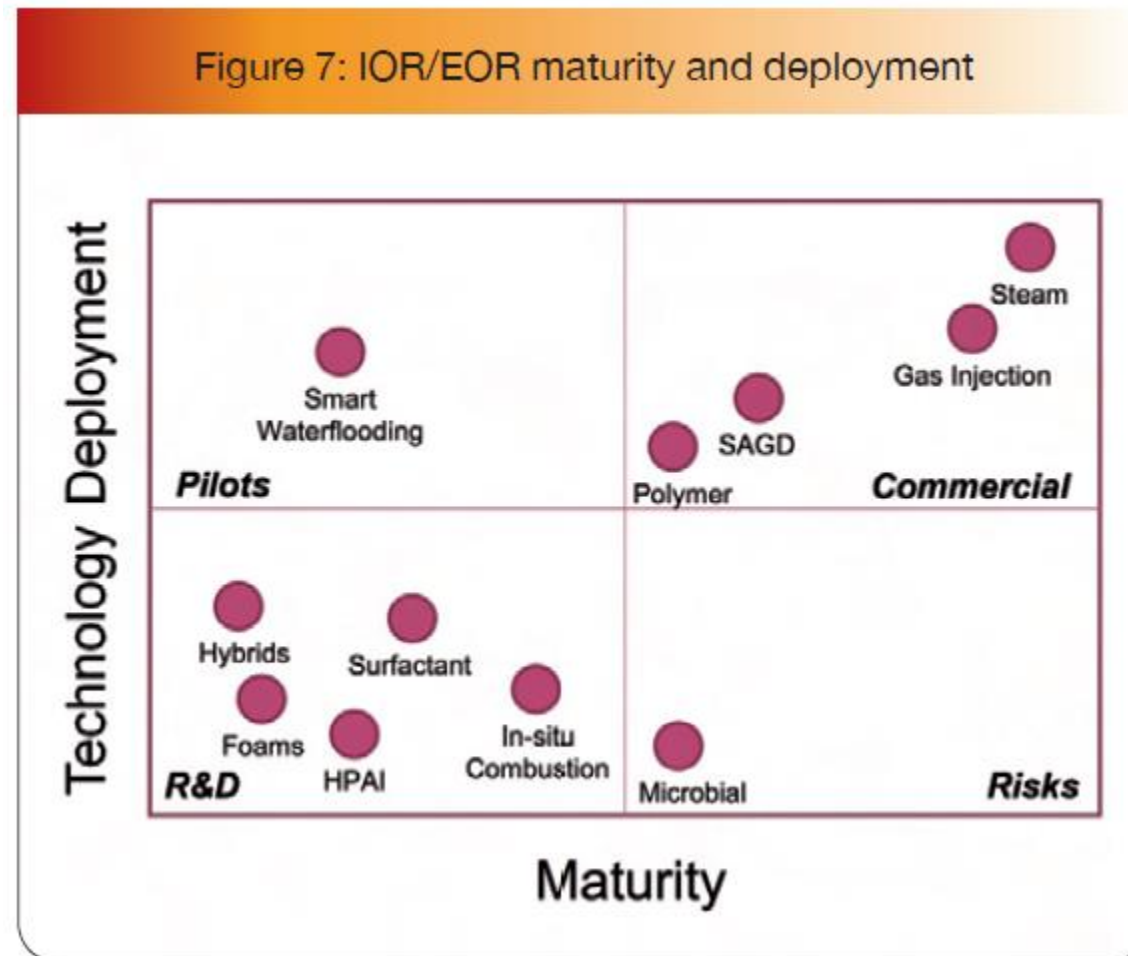
8 Applikationen

8.1 (Surfactant) Enhanced Oil Recovery



8 Applikationen

8.1 (Surfactant) Enhanced Oil Recovery



8 Applikationen

8.1 (Surfactant) Enhanced Oil Recovery

Modifizierte Huminsäure als grenzflächenaktive Substanz

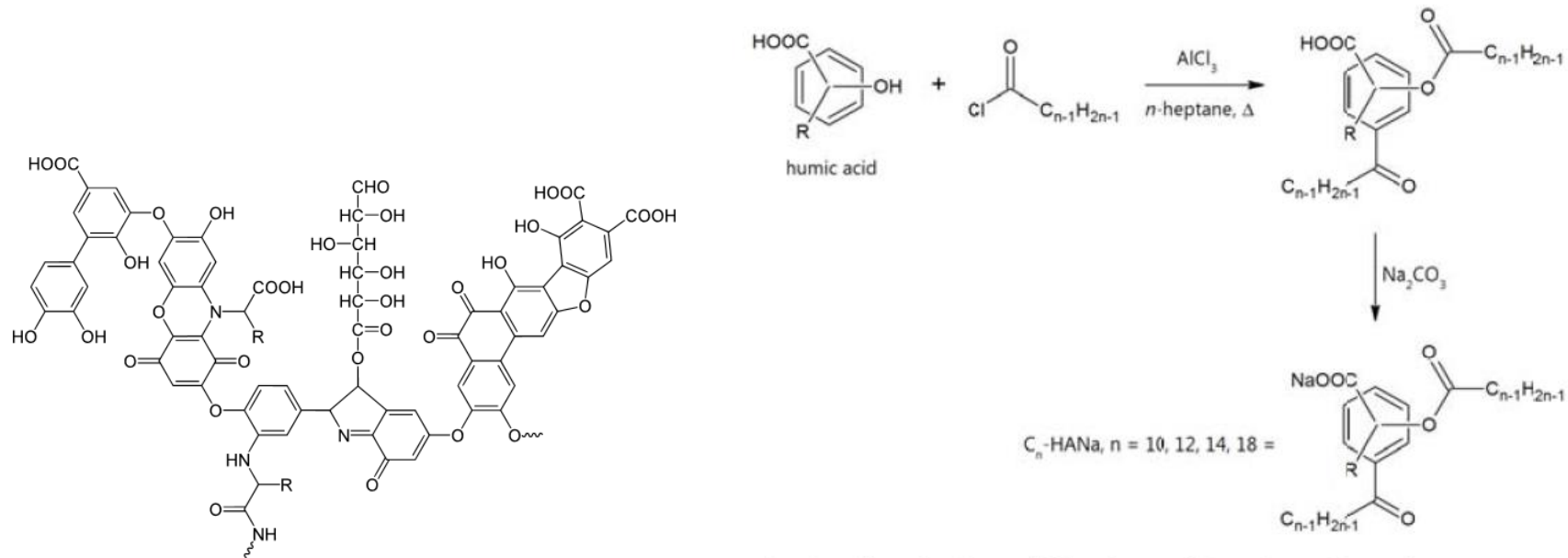


Fig. 2: Chemical modification of humic acid and structure of hydrophobically modified sodium humate (C_n-HANa). Figure as adapted from Ref. [3].

8 Applikationen

8.1 (Surfactant) Enhanced Oil Recovery

Modifizierte Huminsäure als grenzflächenaktive Substanz

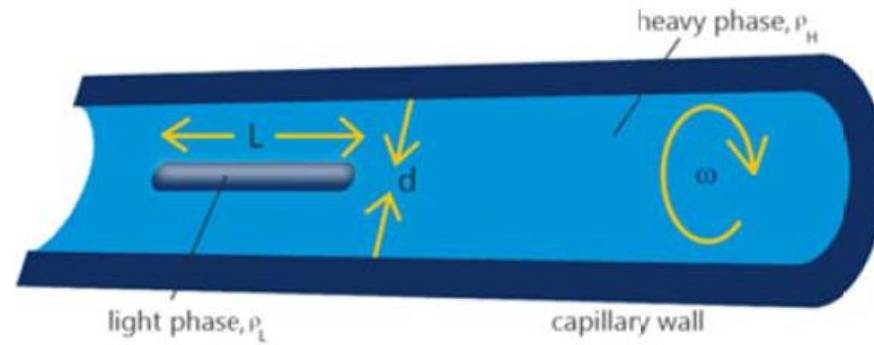


Fig. 3: Schematic setup of a fully prepared glass capillary for spinning drop tensiometry.

$$\gamma = \frac{d^3 \cdot \omega^2 \cdot \Delta\rho}{32}$$

8 Applikationen

8.1 (Surfactant) Enhanced Oil Recovery

Modifizierte Huminsäure als grenzflächenaktive Substanz

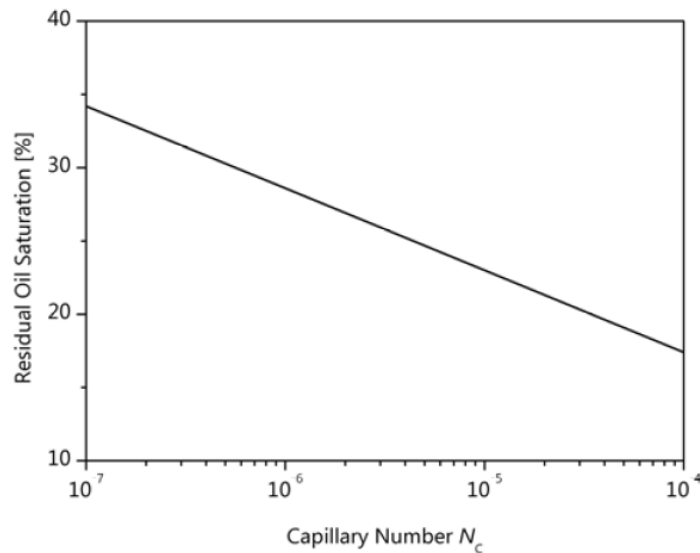


Fig. 1: The residual oil saturation as a function of the capillary number N_c . Decreasing the IFT between displacing fluid and crude oil increases N_c , ultimately lowering the residual oil saturation. Figure as adapted from Ref. [1].

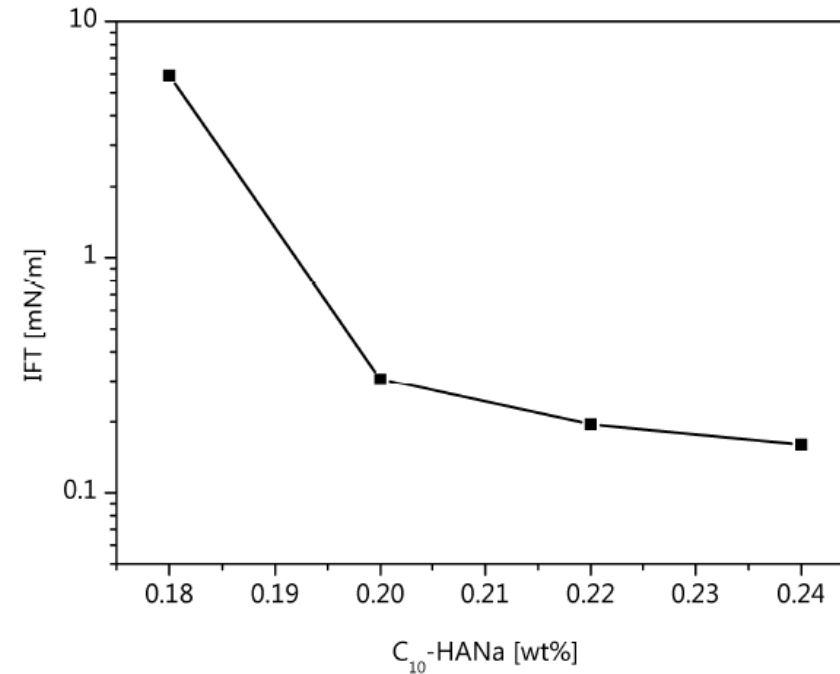


Fig. 4: The IFT between crude oil and aqueous solutions with different concentrations of surfactant C_{10} -HANa. Figure as adapted from Ref. [3]. Data taken with a KRÜSS SITE100.

8 Applikationen

8.1 (Surfactant) Enhanced Oil Recovery

Modifizierte Huminsäure als grenzflächenaktive Substanz

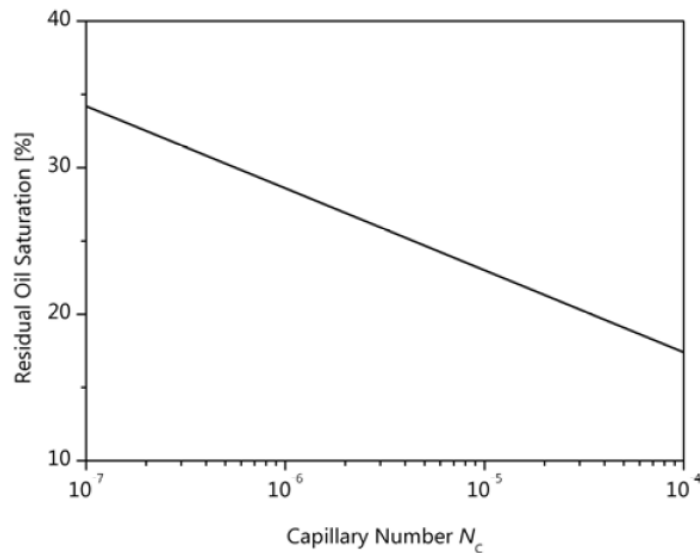


Fig. 1: The residual oil saturation as a function of the capillary number N_c . Decreasing the IFT between displacing fluid and crude oil increases N_c , ultimately lowering the residual oil saturation. Figure as adapted from Ref. [1].

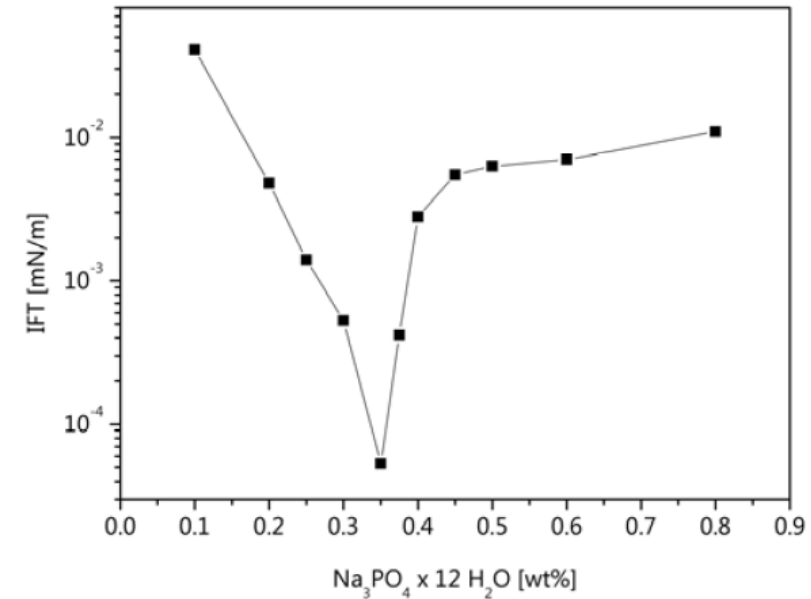


Fig. 5: The influence of chemically modified humic acid (0.12 % C_{12} -HANa) and alcohol (4 % *n*-propanol) on the IFT at different alkali concentrations. Figure as adapted from Ref. [3]. Data taken with a KRÜSS SITE100.

8 Applikationen

8.1 (Surfactant) Enhanced Oil Recovery

Benetzungseinfluss bei Alkali EOR

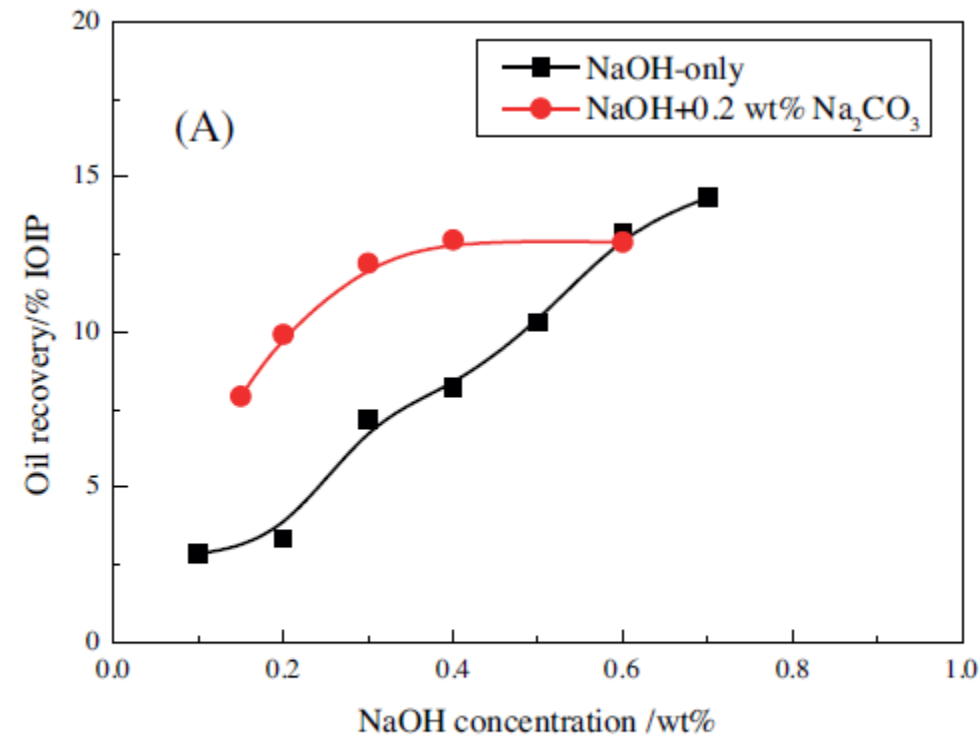


Fig. 3. Effect of NaOH concentration on tertiary oil recovery in alkaline injection.

8 Applikationen

8.1 (Surfactant) Enhanced Oil Recovery

Benetzungseinfluss bei Alkali EOR

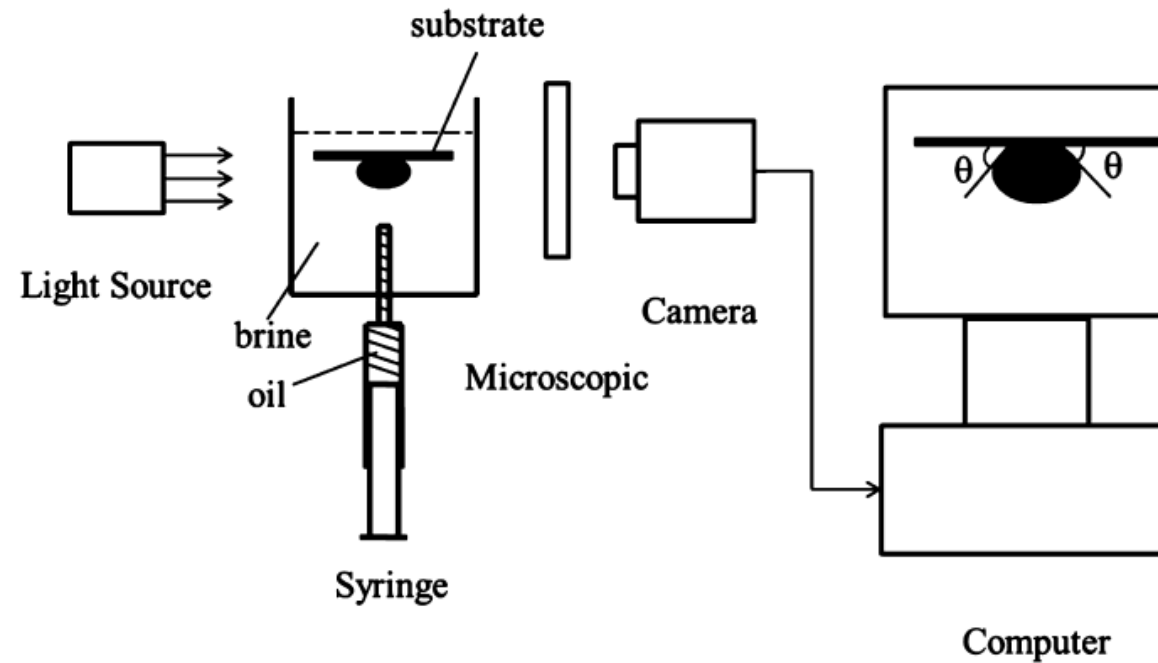


Fig. 2. Schematic diagram of contact angle measurement.

8 Applikationen

8.1 (Surfactant) Enhanced Oil Recovery

Benetzungseinfluss bei Alkali EOR

Table 2
Static contact angles for a heavy oil–brine/ Na_2CO_3 –quartz system.

Contact angle ($^\circ$)	24	42	68	143	167
Concentration (wt%)	0	0.10	0.20	0.30	0.40



Fig. 8. Digital image of sessile oil drops on a quartz substrate, in brine with different NaOH concentrations, at equilibrium state and ambient temperature. (A) 0; (B) 0.1 wt%; (C) 0.2 wt%; (D) 0.3 wt%; (E) 0.4 wt%; (F) 0.5 wt%.

4. Conclusions

The mechanisms and the effects of wettability alteration on the displacement of heavy oil by alkaline flooding have been investigated. The conclusions can be summarized as follows.

- (1) The tertiary oil recovery can be greater than 10% of the initial oil in place (IOIP) by NaOH-only flooding or NaOH and Na_2CO_3 mixed flooding systems.
- (2) The wettability of the pore walls in the micromodel had been changed from water-wet to oil-wet, which can help block water channeling and thereby improve the sweep efficiency.
- (3) Contact angle can be changed from water-wet to oil-wet under the action of NaOH or Na_2CO_3 . The wettability alteration is one of the important mechanisms for enhanced heavy oil recovery by alkaline flooding.

8 Applikationen

8.2 Textilindustrie

Oberflächenenergie

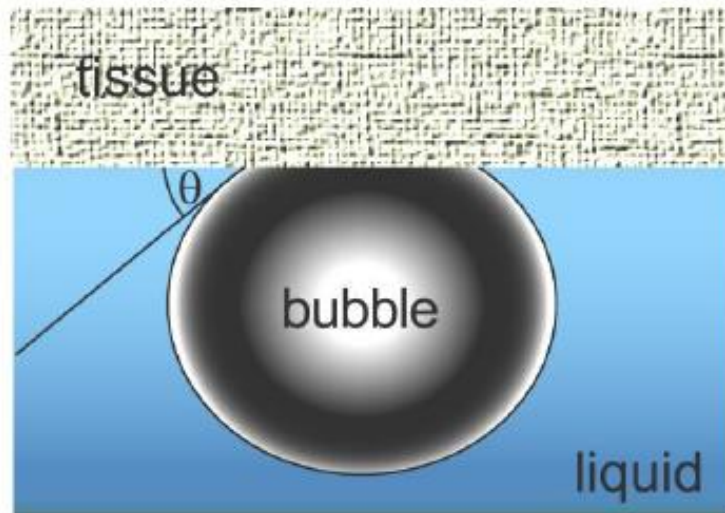


Fig. 1: Schematic view of the captive-bubble arrangement

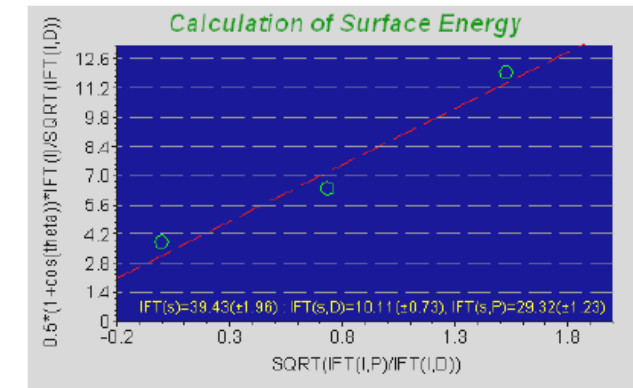
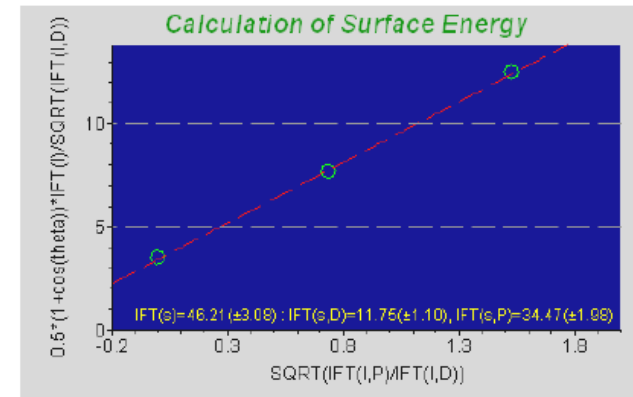


Fig. 2: Evaluation according to OWRK for pure cotton (top) and polymeric compound material (bottom)

	Pure cotton material	Polymeric compound material
Surface energy (mN/m)	46.2	39.4
Polar part (mN/m)	34.5	29.3
Dispersive part (mN/m)	11.7	10.1

Tab. 1: Surface energy of two textile samples

8 Applikationen

8.2 Textilindustrie

Reinigung

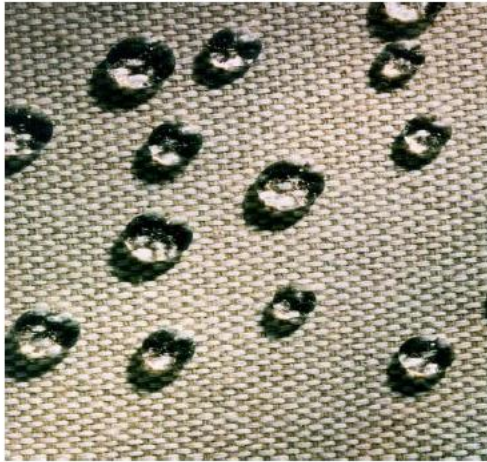


Fig. 1: Drops of water on hydrophobic fabric

Fabric	Contact angle CA (°)
Cotton, scoured	136.1
Cotton, bleached	138.3
Cotton, colored	116.2

Table 1: Static contact angle measurements with water on textile fabrics

Fabric	Contact angle (°)
Cotton, scoured	85.3°
Cotton, bleached	90.1°
Cotton, colored	74.9°

Table 2: Static contact angle measurements with an aqueous surfactant solution (APG 2761, $c_0 = 2.31$ g/l) on textile fabrics

Fabric	Contact angle CA (°)	Free standard wetting enthalpy $\Delta_{\text{Ben}}G^0$ (mJ/m ²)
Cotton, scoured	16.8	-24.18
Cotton, bleached	13.5	-24.56
Cotton, colored	11.5	-24.75

Table 3: Contact angles and free standard wetting enthalpies for textile fabrics with optimized cleaning solution (15% V/V 2-methyl-propanol-(1) + 85% V/V aqueous surfactant solution APG 2761, $c_0 = 7.30$ g/l)